

# Analysis of target multipaths in WiFi-based passive radars

ISSN 1751-8784

Received on 5th February 2015

Revised on 21st May 2015

Accepted on 21st June 2015

doi: 10.1049/iet-rsn.2015.0075

www.ietdl.org

Haroon Mazhar, Syed Ali Hassan ✉

School of Electrical Engineering and Computer Science (SEECS), National University of Sciences and Technology (NUST), Islamabad, Pakistan

✉ E-mail: ali.hassan@seecs.edu.pk

**Abstract:** In this study, the authors investigate the effects on the range measurement accuracy of a WiFi-based passive radar when multiple copies of signal, from the same target, are received due to propagation through a rich-scattering environment. These multipath returns from stationary scatters induced range measurement inaccuracies in passive radars including offset of the target from its true range, smearing of the target in range dimension or appearance of ghost targets. Relationship between range measurement inaccuracies due to target multipaths and range resolution of transmission waveform has been studied. A two-step solution, that is, signal separation followed by equalisation, is also proposed to mitigate the effects of multipaths in WiFi-based passive radars.

## 1 Introduction

Long-range surveillance applications of passive radars, using various analogue and digital waveforms, have reached to a point of maturity and practical systems have started to appear in market for various defence and civil applications, like Silent Sentry by Lockheed Martin, Cellstar by Roke Manor Research Limited, and Homeland Alerter 100 by Thales Group [1]. Owing to the many advantages offered by the passive radars, there is a growing interest to utilise them in urban and indoor sensing environment for the detection of human or vehicular targets. Various digital waveforms including GSM, DVB-T, DAB, WiFi, and worldwide interoperability for microwave access have been analysed by different researchers for feasibility of utilising them as illuminators of opportunity for passive radars [2–6]. The omnipresence of different variants of IEEE 802.11-based wireless local area networking (WLAN) signals make them a suitable transmissions of opportunity for indoor and urban sensing applications of the passive radars. IEEE 802.11 a,b,g, and n standards are most prolific waveforms found in urban environment to provide WLAN connectivity of up to 600 Mbps, using a mix of orthogonal frequency-division multiplexing (OFDM) and direct-sequence spread spectrum (DSSS) modulations in 2.5 and 5 GHz industrial, scientific, and medical (ISM) radio frequency bands.

Active research is going on to utilise the WiFi waveforms for passive radars in urban applications. Colone *et al.* [6] have thoroughly analysed the ambiguity functions of various WiFi standards to determine their suitability for passive radar applications. The research indicates that the range resolution performance is dominated by periodic beacon signals and theoretical range resolution ( $R_{res}$ ) is of the order of 25 m, whereas the velocity resolution of 0.2 m/s can be achieved using a target integration time of 0.6 s, which is reasonable to detect slow moving human targets. Chetty *et al.* [7] have demonstrated low cost through the wall (TTW) passive radar system using WiFi signals to detect human targets from stand-off distances. Colone *et al.* [8] have experimented with WiFi waveforms to detect human and vehicular targets in indoor and outdoor environments; moreover, they applied the inverse synthetic aperture radar technique for detection and tracking of vehicles through high-resolution cross-range profiling [9]. They also addressed the two-dimensional (2D) localisation in a WiFi-based passive radar using multiple receivers in [10].

In a rich-scattering urban environment, the reflected signal from the target can reach the passive radar receiver through multiple paths, because of reflections from surrounding scatter objects. These multiple copies of the signal from the same target combine

vectorially at the receiver to give rise to constructive or destructive interference, which may seriously degrade the range measurement accuracy of the passive radar. In active radars, the multipath errors are sometimes called *low-angle tracking errors*, which arise due to signal bouncing off from smooth ocean or earth surface giving rise to ghost targets [11]. Setlur *et al.* [12, 13] have extensively researched on multipath model, and its further exploitation, in TTW active radars. Researchers have also faced range measurement errors in WiFi-based passive radars due to target multipaths [7, 10]; however, same were ignored in both the works. Although Chetty *et al.* [7] introduced the target multipaths in their initial mathematical model; however, it was neglected to simplify the discussion which resulted in erroneous range measurement in their TTW passive radar experiment.

In a WiFi-based urban sensing passive radar, the multipaths cannot be ignored and will cause range measurement errors. Primary reason is the geometry of the environment, in which all signals are received in a 2D plane where, despite of significant path length difference in-between direct and multipath signals, considerable power is received in multipath signal returns. In contrast, for aerial target detection application, signals are received in 3D due to the height of aircraft and the fact that ground scatter objects do not give rise to multipath as the target receiver antenna is pointed towards sky. In this study, we thoroughly investigate the target multipaths problem in a WiFi-based passive radar and the type of range measurement errors they may introduce. We also propose an equaliser solution to determine the true range of the target in a rich-scattering environment, which is a two-step process as described in the last section of the paper.

## 2 Signal and channel model

To study the effects on range measurement accuracy of passive radar, when multiple delayed copies of signal are received from a target in a rich-scattering environment, 802.11 WLAN signal has been simulated and analysed. IEEE 802.11a standard operates at 5 GHz whereas IEEE 802.11 b and g standards operate at 2.4 GHz ISM frequency bands, with a maximum data rate capacity of 11 Mbps for 802.11b standard and 54 Mbps for 802.11a/g standards, by utilising a mix of DSSS and OFDM modulations and channel bandwidth of 20 MHz [14]. Recently, 802.11n standard has become popular, which can support a maximum data rate of 600 Mbps by utilising multiple-input and multiple-output antennas in

2.4/5 GHz frequency bands, channel bandwidth of 40 MHz and OFDM modulation.

The 802.11 a/b/g WiFi signals are dominated by the beacon signals, which use DSSS modulation and this study is based on using the beacon frames for passive radar application. Beacon frame is a type of management frame, which is periodically transmitted to announce the presence and capabilities of wireless access point (AP). The beacon frames are transmitted at regular intervals using lowest data rate of operating standard of the AP. Each simulated beacon frame contains Physical Layer Convergence Protocol (PLCP) preamble (128 bit long preamble and 16 bit start frame delimiter), 48 bit PLCP header and payload data. The baseband data is modulated at 1 Mbps using differential binary phase shift keying and length 11 Barker code [+1, 1, +1, +1, 1, +1, +1, +1, 1, 1, 1] is later applied to spread the signal [14]. The simulated beacon frames are transmitted on frequency channel 6 (2437 MHz) at an interval of 1024  $\mu$ s. The data set used for passive radar simulation is 10 ms long, which contains five beacon frames each of 0.79 ms and sampling frequency ( $F_s$ ) is set to 88 MHz (sample time  $T_s = 1/F_s$ ).

## 2.1 Ambiguity function analysis

The self-ambiguity function, which is a correlation function of same signal with time delayed and Doppler shifted copies, is used to analyse the suitability of any waveform for radar applications. The ambiguity function of simulated signal is calculated using

$$\chi(\tau, f_D) = \left| \int_{-\infty}^{\infty} u(t)u^*(t - \tau)e^{-2\pi j t f_D} dt \right|^2, \quad (1)$$

where  $u(t)$  is the transmitter waveform,  $\tau$  is the time delay and  $f_D$  is the Doppler frequency. The given equation can be implemented by three approaches namely fast Fourier transform (FFT) method, cross-correlation method and double summation method [15]. The first two approaches require lesser computational power as compared with the third one; however, the main disadvantages of these two are that the ambiguity function will be calculated for all possible  $f_D$  using FFT method and all possible  $\tau$  by using cross-correlation method. In practical applications, evaluation of only a subset of  $\tau$  and  $f_D$  is required depending upon the expected target location, velocity, and transmission characteristics. Hence in this study, double summation method is implemented to evaluate the ambiguity function. It is pertinent to highlight that due to a large number of data points in simulated WiFi beacon signal of 10 ms, it was beyond the capabilities of a normal desktop computer to calculate the ambiguity function; hence 64 cores Solaris Cluster running Matlab 2009 was utilised which is available at the High Performance Computing lab of SEECS, NUST [16].

The ambiguity function of 802.11 WiFi signals has been thoroughly analysed in [6]. The ambiguity function of simulated WiFi beacon signals is shown in Fig. 1. The results are consistent with the study done in [6], which was carried out on actual WiFi 802.11b beacon signals.

## 2.2 Channel model

A propagation channel model is created to simulate the location of targets and multipath scattering objects using

$$h(t) = \sum_{n=1}^N C_n e^{j(\phi_n - 2\pi c \tau_n / \lambda_c + 2\pi f_D \tau_n)} \delta(t - \tau_n), \quad (2)$$

where  $h(t)$  is a channel response,  $C_n$  is the complex gain, which depends on the cross-section area of a target or a scattering object,  $\phi_n$  is the random phase induced on the signal by the reflecting object and assumed to be uniformly distributed between  $[-\pi, \pi]$ ,  $c$  is the speed of light,  $\tau_n$  is the delay due to location of target or multipath scatter,  $\lambda_c$  is the wavelength of the transmitted signal

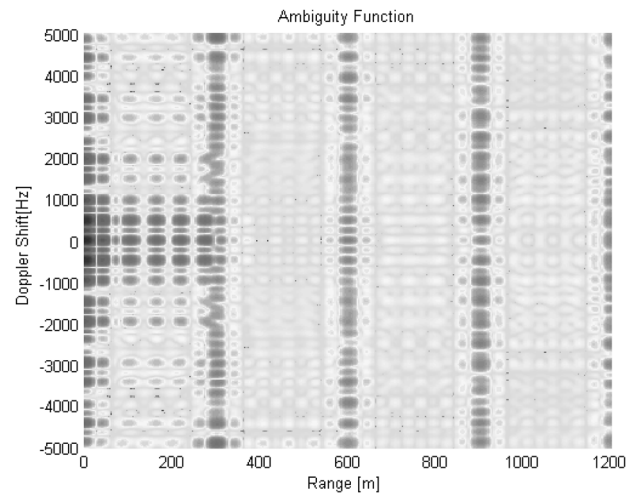


Fig. 1 Self-ambiguity function of WiFi beacon signal

and  $f_D$  is the Doppler frequency induced due to the velocity of target [17]. The total number of reflecting objects is denoted by  $N$ , including both targets and scattering objects, available in the environment. It is assumed that only static scattering objects are present, hence all returns, including direct and multipath, from a single target will have the same Doppler frequency  $f_D$  but will vary in  $\tau_n$  depending on the location of target and multipath scattering objects. The delay  $\tau_n$  corresponds to the bistatic range  $R = c\tau_n$ , implying that it is a sum of distances between transmitter to target and target to receiver for direct target reflection. Moreover, additional multipath length is added in the presence of multipath. The received signal in target channel of the receiver is a convolution of the transmitted waveform and channel response given as

$$s(t) = u(t) * h(t), \quad (3)$$

where  $s(t)$  is the signal received in target channel of passive radar,  $u(t)$  is the transmitted waveform and  $*$  denotes the convolution operator.

## 3 Passive radar processing scheme

In this section, a passive radar processing scheme is introduced, which has been followed to determine the effects of multipath target returns on the range measurement accuracy of a WiFi-based passive radar in an urban environment. Generally, two receiving channels are employed in a passive radar system, one to receive the reference signal and the other to receive the target returns. Subsequently, the cross-correlation between these two signals is evaluated to determine the target range and velocity. In bistatic passive radars, the transmitter is not co-located with the receiver; thus the transmitted signal after passing through wireless channel experiences degradations, hence signal processing is required to be carried out to bring the exact replica of the transmitted waveform, which is to be utilised as a reference signal. The signals received in the reference channel can be defined by following equation

$$r(t) = A_{\text{ref}} u(t - \tau_{\text{ref}}) + \hat{n}(t), \quad (4)$$

where  $r(t)$  is the signal received in the reference channel,  $u(t)$  is the transmitted waveform,  $A_{\text{ref}}$  is the amplitude scaling factor and  $\tau_{\text{ref}}$  corresponds to wave propagation delay, which depends on the distance between transmitter and receiver and  $\hat{n}(t)$  is the additive noise in receiving channel. The signal received in target channel is

given as

$$s(t) = \sum_{l=1}^L A_l u(t - \tau_l) e^{j2\pi f_{D_l} t} + \sum_{l=1}^L \sum_{m=1}^M A_{l_m} u(t - \tau_{l_m}) e^{j2\pi f_{D_l} t} + \sum_{c=1}^C A_c u(t - \tau_c) + A_{\text{DSI}} u(t - \tau_{\text{DSI}}) + \hat{n}(t), \quad (5)$$

where  $A$ ,  $\tau$  and  $f_D$ , with their given subscripts are corresponding amplitude scaling factors, time delays and Doppler frequencies, respectively. The first term in (5) corresponds to  $L$  targets to be detected by passive radar each having a bistatic range equivalent to  $c\tau_l$  and target velocity which induces Doppler frequency  $f_{D_l}$ . The second term corresponds to  $M$  multipaths encountered by signal after reflecting from  $L$  targets before reaching the passive radar target channel. In other words, the signal from each target is received through  $M$  multipaths. The next two terms correspond to the reflections from  $C$  stationary clutters and direct signal interference (DSI), respectively. The presence of these two terms is one of the sources of performance degradation in passive radars.

It is to be noted that the received signal from any target is the vector combination of specular target return and the multipath signals, hence the target signal will experience distortion, which will depend on a number of factors including

- (i) location of scattering objects or the extra distance multipath signals have to travel,
- (ii) signal attenuation experienced by multipath signals after reflection,
- (iii) the random phase,  $\phi$ , induced by the scattering objects,
- (iv) the Doppler frequency of the target.

The target bistatic range and Doppler frequency are determined using cross-correlation function between  $s(t)$  and  $r(t)$  as follows

$$\chi[\tau, f_D] = \left| \sum_{n=0}^{N-1} s[n] r^*[n-i] e^{-2\pi j n f_D / F_s} \right|^2, \quad (6)$$

where  $N$  is the total number of samples collected which corresponds to a target integration time of  $NT_s$  and  $i$  is the time bin corresponding to time delay  $\tau = iT_s$ .

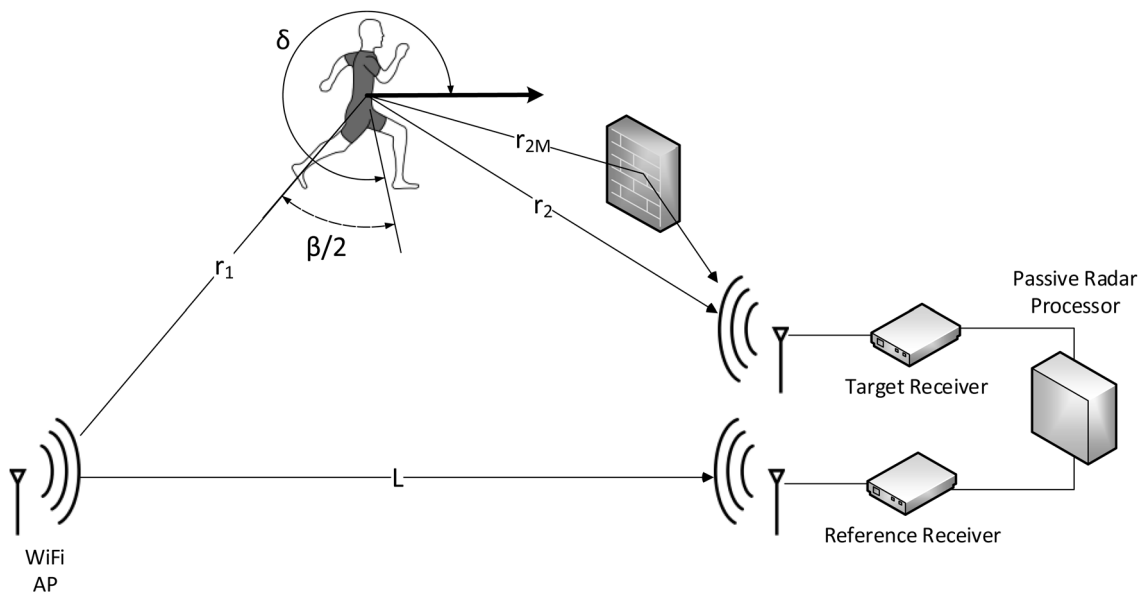


Fig. 2 Target environment model

## 4 Simulation setup and results

To accurately determine the effects of multipaths on the range measurement capability of an urban WiFi-based passive radar, target environment shown in Fig. 2 has been simulated. In the current setup,  $r_1 + r_2$  is the target bistatic range of a single target present in the environment which is 68.18 m, whereas  $r_1 + r_{2M}$  is the bistatic range for the multipath target return. The target velocity  $v$  is 2.5 m/s, signal wavelength  $\lambda$  is 0.123 m, bistatic angle  $\beta$  is  $80^\circ$ , and angle  $\delta$  is  $230^\circ$ . The bistatic Doppler frequency is 20 Hz as calculated using the equation

$$f_D = \frac{2v \cos(\beta/2) \cos(\delta)}{\lambda}. \quad (7)$$

The cross-ambiguity function of this setup is calculated using (6) and is depicted in Fig. 3. The presence of signal target is observed at 68.1 m and 20 Hz Doppler frequency, whereas DSI and static clutter return are at 0 Hz Doppler. As mentioned earlier, the presence of DSI and stationary clutter returns degrade the detection performance of passive radars; however, active research has been done in this area to counter their effects. A comparison of various clutter cancellation techniques is given in [18], which shows that by using various adaptive cancellation algorithms, clutter attenuation in the range of 55–63 dB can be achieved. Colone *et al.* [19] have developed a multistage algorithm, which effectively removes the disturbance from DSI and clutter returns, as well as, enhances the target detection of weaker targets. Furthermore, spatial suppression of DSI signal can also be achieved by using directional antennas directed towards the area of surveillance. In a similar work like this one [7], researchers have practically used CLEAN algorithm which iteratively subtracts the DSI and clutter components from range–Doppler surface to nullify their effects. On the basis of this research, in this study the attenuated DSI and static clutter signals were added to the signal in target channel such that they do not degrade the target detection capability of a WiFi-based passive radar.

To observe the effects on range measurement accuracy of the simulated model, the scatter object was moved to various distances. The cross-ambiguity function in (6) is shown in Fig. 4 at 20 Hz Doppler cut for various positions of the scattering object. The solid plot depicts the range measured in the absence of any multipath whereas the dotted plot is the error induced when signal also travels through a multipath after reflection from the static scattering object. The range resolution ( $\Delta R$ ) grid lines, which

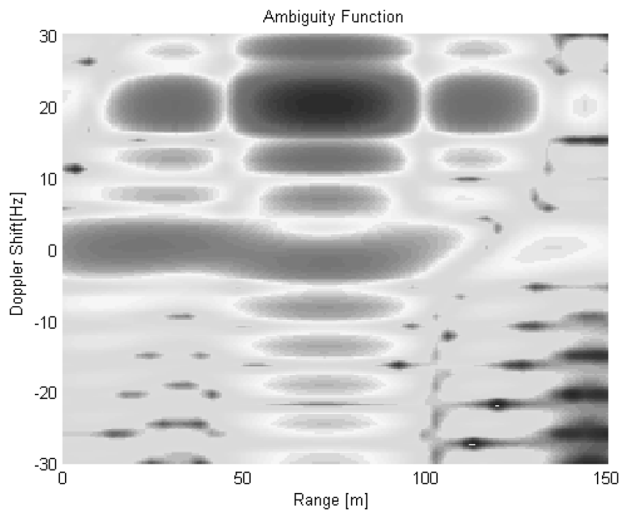


**Fig. 3** Two-dimensional cross-ambiguity function of the simulation environment

correspond to range bins, are also shown in Fig. 4. As a result of distorted target signal, the resultant target range peak will either be *offset* from the true range (Fig. 4a) or the target will *smear* in

range dimension (Fig. 4b) or *ghost* targets will appear, which may not necessarily correspond to actual specular or multipath length (Fig. 4c). In case of smearing of target sufficient energy will spill over to adjacent range bin only, whereas ghost target will always appear further away from adjacent range bin. However, the resultant range plot, among depicted plots, will be temporal due to the movement of target since small change in the location of target will result in large phase variation for both direct and multipath signal [17].

The appearance of offset, smeared or ghost target in range dimension of ambiguity plot is also dependent on path length difference between the direct and reflected signal path and has been analysed in relation to radar range resolution ( $R_{res}$ ). On the basis of the number of simulation runs, it has been observed that, if  $\Delta R < R_{res}$  or  $R_{res} < \Delta R < 2R_{res}$  all three types of range distortion may appear (Figs. 4a–c), however in case of  $\Delta R > 2R_{res}$  ghost targets will only appear, as shown in Fig. 4c.

Another scenario is also considered, when two targets are present in a rich-scattering environment, as depicted in Fig. 5. One target, having 70 Hz Doppler, is at 770 m with two multipaths at  $\Delta R_1 = 10$  and  $\Delta R_2 = 20$  m; whereas other target is at 550 m with a Doppler frequency of  $-50$  Hz, having only strong specular component and no multipath reflections. It has been observed that the given high Doppler resolution is achieved using long target integration time; multipaths arising from one target do not influence the range measurement accuracy of other targets.

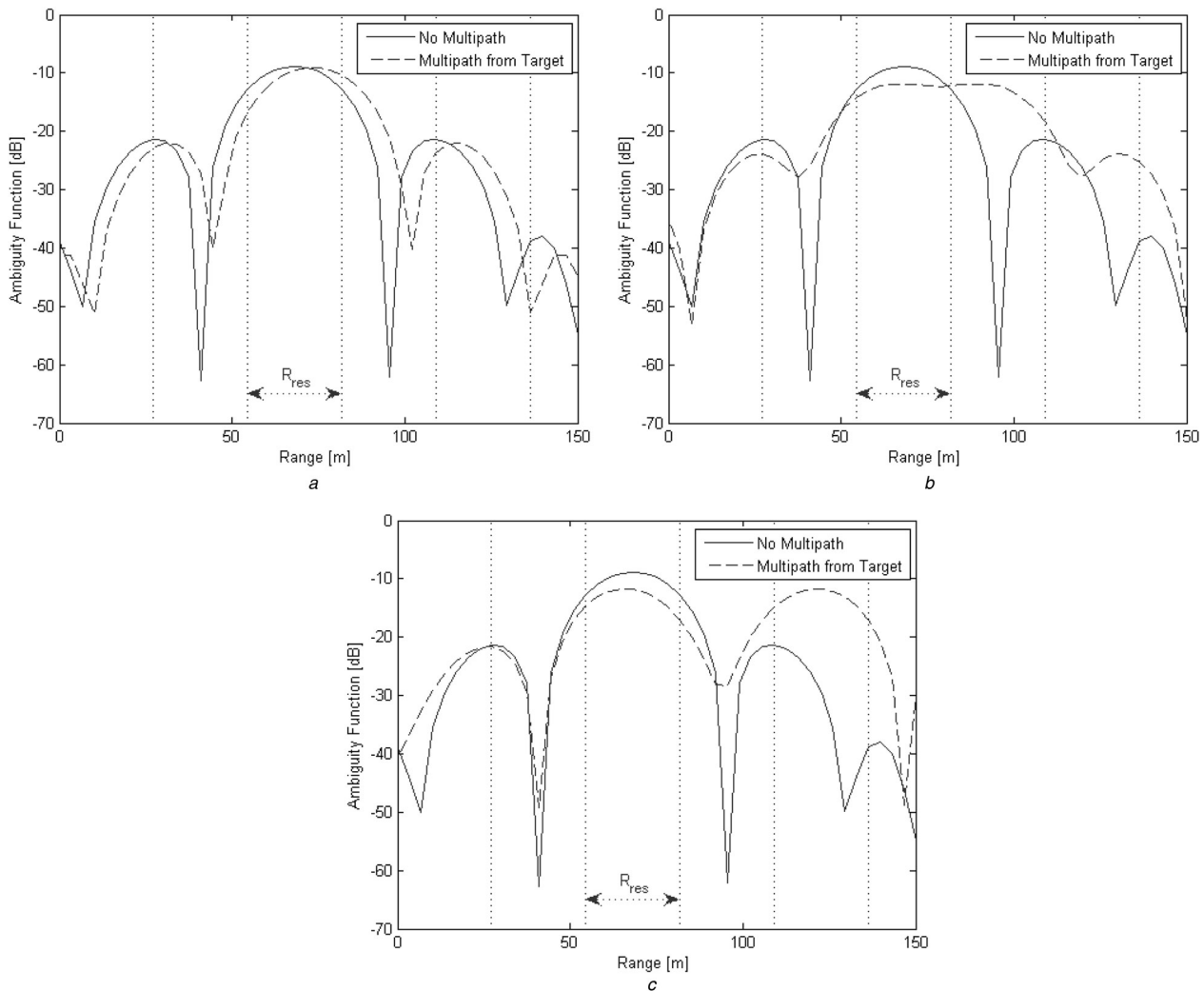


**Fig. 4** Range measurement inaccuracies as a result of multipath

- a Target offset in range
- b Target smeared in range
- c Appearance of ghost target

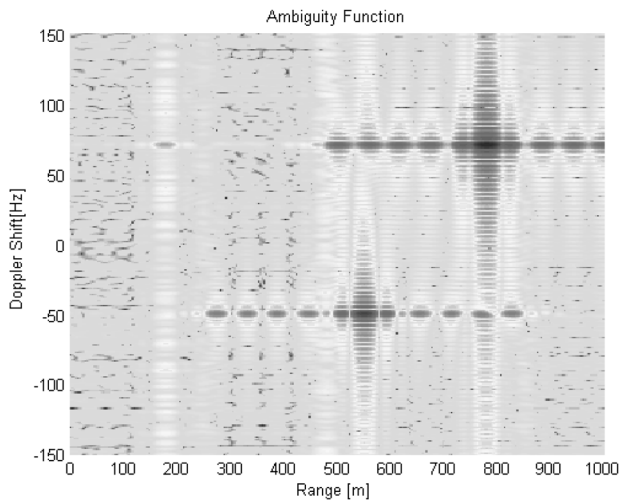


**Fig. 5** Two-dimensional cross-ambiguity function when two targets are present in environment

## 5 Equalisation for target multipath

On the basis of the results of previous section and experiments of other researchers [7], it has been established that the target multipaths seriously degrade the performance of WiFi-based passive radar in urban sensing environment. However, equalisation of target multipaths is not a straightforward problem due to multiple challenges. The wireless propagation channel cannot be known in advance, as all the targets in the environment are, in fact, the moving scatter objects; moreover, this channel is time varying due to the movement of targets. Signal received in the target channel of passive radar is a linear combination of all target returns and associated multipaths (5). In other words,  $h(t)$  in (2) is the aggregate channel response of all targets. As each target along with its associated multipaths presents a different channel to the receiver, signal returns associated with the target of interest are required to be extracted from  $s(t)$  and then equalised to determine the true range of that target. On the basis of this discussion, the equalisation problem can be divided into two steps:

- (i) Separation of direct and multipath signals, of target of interest, from aggregate signal received.
- (ii) Equalisation of extracted signal to determine the true range of target.

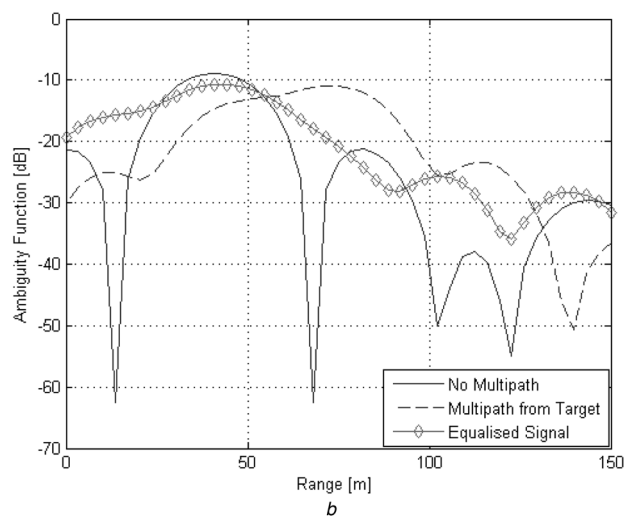
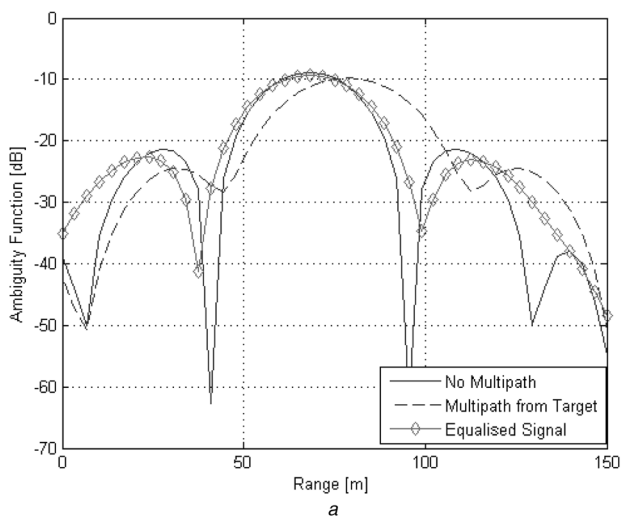


**Fig. 6** Ambiguity function after target equalisation

- a Offset target equalised
- b Smear target equalised

Step 1, although not a simple problem in itself, can be done using advance signal processing techniques like blind signal separation (BSS) [20] or adaptive beam forming of the receiver antenna towards target of interest. For step 2, linear equaliser – which is an adaptive equalisation technique when propagation channel is unknown – can be used to correct the target ranges. Digital waveforms commonly used in urban applications of passive radars contain a known training sequence, which is transmitted in the packet header to combat the inter symbol interference. These training symbols are used as a reference for equalisation process thus to mitigate the effects of multipaths. In 802.11b WiFi signals, 128 bits long preamble or 56 bits short preamble is transmitted in every packet as a known training sequence. It is reiterated that adaptive equalisation process cannot be applied before carrying out step 1 if more than one target is present in an environment, as in Fig. 5, because the equaliser will treat all targets as scatter objects that give rise to multipaths.

Equalisation process was applied to the simulation setup presented in the previous section. An eight tap symbol spaced adaptive linear equaliser [17], based on least mean square algorithm with a step size of 0.02, was applied to the received signal, using long preamble as a training sequence. The target range correction result is shown in Fig. 6a. The target was actually present at 68.1 m, however when multipath signal from  $\Delta R = 20.45$  m was also received along with the direct signal, the measured range was offset to 78.4 m. The linear equaliser corrected the targets to its true range, which is shown as red plot. Similarly, equalisation process was also applied to another scenario where single target was present at 40.9 m, which was smeared in range due to multipaths. The range correction by equalisation is shown in red plot of Fig. 6b.

It is to be noted that the target detection process has now been divided into two phases. In the first phase, coarse target ranges and velocities of all available targets in the environment are calculated using a 2D cross-ambiguity function. This coarse target information is then utilised in the second phase to separate the targets of interest from the composite received signal. The separated signal of each target of interest is processed through independent equalisation processes to determine the true ranges using 1D cross-ambiguity function matched to the Doppler frequency of the target of interest. The signal flow diagram for target detection in two phases is shown in Fig. 7. The reference signal is equalised to bring out the exact replica of the transmitted signal and subtracted from the target channel signal to remove DSI and static clutter at 0 Hz Doppler frequency. A 2D cross-ambiguity function (6) is calculated, followed by a detection algorithm to determine the coarse location and Doppler frequency of the targets available in the environment. On the basis of the

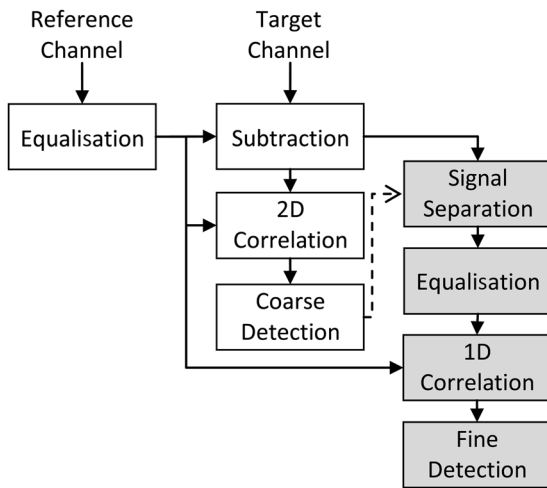


Fig. 7 Process diagram for target detection in two phases

coarse detection information, signal from targets of interest are separated and equalised to mitigate the effects of multipaths. One-dimensional cross-correlation function of the equalised signal is calculated and true range of the target under evaluation is determined by a fine detection algorithm. To further comment, if the targets of interest are separated through antenna beam forming, the targets can be localised using direction of arrival of signal, whereas if step 1 is carried through BSS, the corrected ranges may be passed to central processing station of multistatic passive radar system to determine the location of the targets of interest [10].

Keeping above in view, a study is under progress to blindly separate the signals of targets of interest, for further equalisation, from composite received signal using higher-order statistics. Moreover, as a future work, the simulation results and performance of the proposed scheme shall also be verified through hardware experiments.

## 6 Conclusions

In urban sensing application of passive radars, multiple copies of target echoes can be received due to signal travelling through multipaths in a rich-scattering environment. These target multipaths seriously degrade the range measurement accuracy, which results in target either offsetting from actual range, smearing in range dimension or ghost targets may appear, depending on the range resolution of the selected waveform and relative path difference of multipath to direct signal path. It was observed that if the relative path difference is less than twice the range resolution, all three range degradation may appear, whereas only ghost targets will appear if the path difference is greater than double the range resolution.

It has been proposed that target detection should be carried out in two phases, namely coarse detection and fine detection. For fine detection of targets in a rich-scattering environment, it has been demonstrated that a two-step equalisation process can accurately determine the true range of the targets, which may be utilised for target localisation.

## 7 References

- Palmer, J., Palumbo, S., Summers, A., Merrett, D., Searle, S., Howard, S.: 'An overview of an illuminator of opportunity passive radar research project and its signal processing research directions', *Def. Appl. Signal Process*, 2009, **21**, (5), pp. 593–599
- Tan, D.K.P., Sun, H., Lu, Y., Lesturgie, M., Chan, H.L.: 'Passive radar using global system for mobile communication signal: theory, implementation and measurements', *IET Radar Sonar Navig.*, 2005, **152**, (3), pp. 116–123
- Coleman, C.J., Watson, R.A., Yardley, H.: 'A practical bistatic passive radar system for use with DAB and DRM illuminators'. Proc. IEEE Radar Conf., Rome, Italy, 2008
- Colone, F., Langellotti, D., Lombardo, P.: 'DVB-T signal ambiguity function control for passive radars', *IEEE Trans. Aerosp. Electron. Syst.*, 2014, **50**, (1), pp. 329–347
- Colone, F., Falcone, P., Lombardo, P.: 'Ambiguity function analysis of WiMAX transmissions for passive radar'. Proc. IEEE Radar Conf., 2010, pp. 689–694
- Colone, F., Woodbridge, K., Guo, H., Mason, D., Baker, C.J.: 'Ambiguity function analysis of wireless LAN transmissions for passive radar', *IEEE Trans. Aerosp. Electron. Syst.*, 2011, **47**, (1), pp. 240–264
- Chetty, K., Smith, G.E., Woodbridge, K.: 'Through-the-wall sensing of personnel using passive bistatic WiFi radar at standoff distances', *IEEE Trans. Geosci. Remote Sens.*, 2012, **50**, (4), pp. 1218–1226
- Colone, F., Falcone, P., Bongioanni, C., Lombardo, P.: 'WiFi -based passive bistatic radar: data processing schemes and experimental results', *IEEE Trans. Aerosp. Electron. Syst.*, 2012, **48**, (2), pp. 1061–1079
- Colone, F., Pastina, D., Falcone, P., Lombardo, P.: 'WiFi-based passive ISAR for high-resolution cross-range profiling of moving targets', *IEEE Trans. Geosci. Remote Sens.*, 2014, **52**, (6), pp. 3486–3501
- Falcone, P., Colone, F., Macera, A., Lombardo, P.: 'Two-dimensional location of moving targets within local areas using WiFi-based multistatic passive radar', *IET Radar Sonar Navig.*, 2014, **8**, (2), pp. 123–131
- Skolnik, M.: 'Radar handbook' (McGraw-Hill, 2008, 3rd edn.)
- Setlur, P., Amin, M., Ahmad, F.: 'Multipath model and exploitation in through-the-wall and urban radar sensing', *IEEE Trans. Geosci. Remote Sens.*, 2011, **49**, (10), pp. 4021–4034
- Setlur, P., Alli, G., Nuzzo, L.: 'Multipath exploitation in through-wall radar imaging via point spread functions', *IEEE Trans. Image Process.*, 2013, **22**, (12), pp. 4571–4586
- IEEE 802.11 Working Group: 'Wireless LAN medium access control (MAC) and physical layer (PHY) specifications', 1997
- Johnson, J.J.: 'Implementing the cross ambiguity function and generating geometry-specific signals', MS thesis, Naval Postgraduate School Monterey CA, 2001
- HPC Lab, SEECS, NUST. Available at <http://www.hpc.seecs.edu.pk/hardware.php>, accessed 1 February 2015
- Stuber, G.L.: 'Principles of mobile communication' (Springer, 2012, 3rd edn.)
- Cardinali, R., Colone, F., Ferretti, C., Lombardo, P.: 'Comparison of clutter and multipath cancellation techniques for passive radar'. Proc. IEEE Radar Conf., 2007, pp. 469–474
- Colone, F., O'hagan, D.W., Lombardo, P., Baker, C.J.: 'A multistage processing algorithm for disturbance removal and target detection in passive bistatic radar', *IEEE Trans. Aerosp. Electron. Syst.*, 2009, **45**, (2), pp. 698–722
- Belouchrani, A., Abed-Meraim, K., Cardoso, J.F., Moulines, E.: 'A blind source separation technique using second-order statistics', *IEEE Trans. Signal Process.*, 1997, **45**, (2), pp. 434–444